1 **Observation of regional air pollutant transport between the**

2 **megacity Beijing and the North China Plain**

3 Yingruo Li[1], Chunxiang Ye[1,2], Jun Liu[1], Yi Zhu[1], Junxia Wang[1], Zhiqiang Tan[1], Weili Lin[3],

4 Limin Zeng[1], Tong Zhu[1,4*]

5 [1]State Key Laboratory of Environmental Simulation and Pollution Control, College of

6 Environmental Sciences and Engineering, Peking University, Beijing, 100871, China

7 [2]Now at School of Chemistry, University of Leeds, Leeds LS2 9JT, UK

8 [3]Meteorological Observation Center, China Meteorological Administration, Beijing,

9 100081, China

10 [4]The Beijing Innovation Center for Engineering Science and Advanced Technology,

11 Peking University, Beijing, 100871, China

12 *Corresponding Author: tzhu@pku.edu.cn

18 **Abstract.** Megacities have strong interactions with the surrounding regions through

19 transport of air pollutants. It has been frequently addressed that the air quality of

20 Beijing was influenced by the influx of air pollutants from the North China Plain (NCP).

21 However, estimations of air pollutant transport between megacities and surrounding

22 regions using long–term observations are very limited. Using the observational

23 results of the gaseous pollutants SO_2, NO, NO_2, O_3, and CO from August 2006 to

24 October 2008 at the Yufa site, a rural site south of Beijing, together with

25 meteorological parameters, we evaluated the transport flux between Beijing and the

26 NCP, as part of the "Campaign of Air Quality Research in Beijing and Surrounding

27 Region 2006–2008" (CAREBeijing 2006–2008). The bivariate polar plots showed the

28 dependence of pollutant concentrations on both wind speed and wind direction, and

29 thus inferred their dominant transport directions. Surface flux calculations further

30 demonstrated the transport directions and the seasonal variations in the cumulative

31 transport strengths. The cumulative transport strengths of SO_2, NO, NO_2, NO_x ($NO_x =$

32 $NO + NO_2$), O_3, O_x ($O_x = O_3 + NO_2$), and CO were 92.6, –62.2, –8.9, –71.0, 217.3, 213.8,

33 and 1038.1 $mg\ s^{-1}\ m^{-2}$ during the observation period, respectively. For SO_2, CO, and

34 O_3, the transport fluxes were from the NCP to Beijing in all seasons except winter,

35 with the strongest fluxes largely in summer. The transport flux of NO_x was from

36 Beijing to the NCP except in summer, with the strongest flux in winter. Finally, our

37 analysis suggests a profound influence of regional transport between Beijing and the

38 NCP on the air quality of the megacity Beijing. Our study also suggested that various

39 factors, such as the wind field, emission inventory, and photochemical reactions,

40 could influence the transport of air pollutants between Beijing and the NCP.

41 Therefore, both local emission reduction and regional cooperation must be

42 considered in air quality management of the megacity Beijing.

43 **Keywords:** Megacity Beijing, North China Plain, Yufa site, Regional transport, Long-

44 term and multiple-species observation

45 **1. Introduction**

46 Megacities are large sources of air pollutants and greatly influence the surrounding

47 areas (Parrish and Zhu, 2009). With a population over 20 million, the city of Beijing is

48 an example of such a megacity. Beijing has faced severe air pollution problems over

49 the past two decades and has intensive interactions with other emission hot spots

50 within the North China Plain (NCP) (Shao et al., 2006; Zhang et al., 2012). Beijing and

51 the NCP are surrounded by the Yanshan Mountains to the north and the Taihang

52 Mountains to the west. The semi-basin geographical features together with

53 continental monsoon climate (Xu et al., 2005) make regional transport of air

54 pollutants between the megacity Beijing and the NCP important factors affecting air

55 quality in Beijing and the NCP (An et al., 2007; Guo et al., 2010; Lin et al., 2008, 2009;

56 Streets et al., 2007; Wang et al., 2006; Wang et al., 2011; Wu et al., 2011; Xu et al.,

57 2011). An improved understanding of the regional transport of air pollutants

58 between Beijing and the NCP is therefore essential for air quality management of the

59 megacity Beijing and establishment of regional-scale emissions control measures.

60 Previous studies have shed light on the regional transport sources of the

61 megacity Beijing, and various techniques, including rural/urban stationary

62 observations (Guo et al., 2010; Lin et al., 2008, 2009; Wang et al., 2006; Xu et al.,

63   2011), mobile laboratory measurements (Wang et al., 2009, 2011), and modelling

64   studies (An et al., 2007; Matsui et al., 2009; Wu et al., 2011), have been employed. A

65   stationary observation (Lin et al., 2009) from July 2006 to September 2007 at the

66   Gucheng site, a rural site south-west of Beijing, found that high concentrations of

67   gaseous pollutants, including NO_x, SO_2, CO, O_3, and O_x, were accompanied by air

68   masses moving northward from Gucheng to Beijing, according to back-trajectory

69   analysis. Similar to Lin et al. (2009), regional transport of air pollutants between

70   Beijing and the NCP was observed consistently in these previous studies (Lin et al.,

71   2008; Yuan et al., 2009; Zhu et al., 2011), even though they were merely short-term

72   observations.

73   Many studies have also attempted to quantify transport fluxes of the main

74   gaseous pollutants. A mobile laboratory study (Wang et al., 2011) in Beijing city

75   demonstrated regional transport of SO_2 from the NCP in both emission-control and

76   non-control scenarios during the Beijing 2008 Olympics. Extrapolated from five 1-day

77   case studies, the annual transport fluxes of SO_2 through the south-east part of the

78   6th Ring Road into Beijing were estimated at 49.2 Gg yr^{-1} and 146.3 Gg yr^{-1},

79   accounting for 70 % and 73 % of the annual SO_2 emissions in Beijing under emission-

80   control and non-control scenarios, respectively. The Community Multi-scale Air

81   Quality (CMAQ) model simulation, which used the emission switch on/off method,

82   found that regional transport of SO_2 and $PM_{2.5}$ from the south-east to Beijing was up

83   to 26 % and 15 %, respectively, and that of PM_{10} reached 60 % in a heavy pollution

84   episode in the spring of 2005 (An et al., 2007). Similarly, the Models-3/CMAQ model

85   simulation over the Beijing region for July 2001, reported by Streets et al. (2007),

86 illustrated the regional transport of secondary $PM_{2.5}$ and O_3 between Beijing and the

87 NCP. The study suggested that the average contributions of regional transport from

88 Hebei, Shandong, and Shanxi in the NCP to $PM_{2.5}$ concentrations in the megacity

89 Beijing were about 32 %, 11 %, and 3.5 %, with maximum contributions of 70 %, 63 %,

90 and 21 %, respectively. The regional transport contributions to the concentrations of

91 O_3 in Beijing were less significant, with maximum contributions of 28 %, 24 %, and 10 %

92 from Hebei, Shandong, and Shanxi, respectively.

93   In summary, long-term observation of transport flux is necessary to constrain

94 regional models and to directly evaluate the influence of regional transport on air

95 quality in the megacity Beijing, as transport flux varies with multiple factors, such as

96 wind vector and pollutant concentrations, which usually show seasonal variations. In

97 this study, we performed quantitative analysis of the surface fluxes of major gaseous

98 pollutants, including SO_2, NO, NO_2, NO_x, O_3, O_x, and CO, based on a 2-year

99 observation at the Yufa site in a rural area south of Beijing. The results showed

100 different transport directions of the main pollutants and seasonal variations in the

101 transport flux strengths. Discussion of the key factors controlling regional transport is

102 important for the establishment of air quality control policy in future.

103 **2. Measurements and Methods**

104 **2.1. Measurements**

105 The Yufa site is suitable for regional transport investigation between the megacity

106 Beijing and the NCP, as it is located along the air pollution route influenced by

107 emissions from the megacity Beijing and long-range transport from the NCP. The

108   measurements at the Yufa site (39°30'49"N, 116°18'15"E) were conducted from the

109   top of a building (about 20 m above ground level) on the campus of Huangpu

110   College. This is a rural site about 50 km south of the centre of Beijing and near the

111   border of Beijing Municipality and Hebei Province. As shown in Fig. 1, the northern

112   and western sides of the site can be influenced by the dry and clean air mass from

113   the mountain area, whereas the southern and south-eastern sides are surrounded by

114   heavily industrialised and urbanised areas, such as Hebei Province and Tianjin City.

115   Detailed site information and emission sources for the Yufa site were reported

116   previously (Takegawa et al., 2009).

117   Figure 1. here

118   The gaseous pollutant species measured included SO_2, NO, NO_2, NO_x, O_3, O_x, and

119   CO. Sulphur dioxide (SO_2) was measured using a sulphur dioxide analyser (9850B;

120   Ecotech, Knoxfield, Australia). Reactive nitrogen species (NO, NO_2, and NO_x) were

121   measured using NO–O_3 chemiluminescence (9841B; Ecotech). Carbon monoxide (CO)

122   was measured using a CO analyser (EC9830A; Ecotech), and Ozone (O_3) was

123   measured using an O_3 analyser (9810B; Ecotech). Measurements of meteorological

124   parameters, including wind direction (WD), wind speed (WS), temperature (T),

125   barometric pressure (BP), and relative humidity (RH), were conducted with a LASTEM

126   auto meteorology station (M7115; LSI-LASTEM, Milan, Italy). All trace gas

127   instruments were maintained and calibrated routinely. The main reasons for missing

128   data were power and instrument failure.

2.2. Methods

2.2.1. Transport direction analysis

The transport of gaseous pollutants is markedly influenced by meteorological parameters, especially wind speed and wind direction. For local emission sources, wind can facilitate the dilution and diffusion of air pollutants. Strong wind usually has marked diffusion capability, whereas weak wind usually leads to accumulation of air pollutants. For regional sources, strong wind can transport pollutants over long distances and may result in high concentrations of pollutants in downwind areas. Therefore, the relationship between pollutant concentration and wind field is an indicator of regional transport.

The bivariate polar plot graphical technique was used to investigate the relationships between the concentrations of gaseous pollutants and wind field, and to identify potential emissions sources and transport directions of air pollutants according to the technique developed by Carslaw et al. (2006) and Westmoreland et al. (2007). The variables (such as pollutant concentrations, wind speed, and wind direction) were plotted in polar coordinates. The procedure was as follows. First, the concentration data were partitioned into wind speed–wind direction bins, and the mean concentrations were calculated within each bin. Then, the wind components u and v were calculated using Eq. (1):

$$u = \mathrm{WS} \cdot \sin(\pi\theta/180), v = \mathrm{WS} \cdot \cos(\pi\theta/180) \quad (1),$$

where WS is the hourly mean wind speed, and θ is the wind direction in degrees, with 90° being from the east. Then, a generalised additive model (GAM;

151   Jayamurugan et al., 2013) was used for surface fitting to describe the concentration

152   as a function of the wind components u and v. The concentrations calculated by the

153   GAM can be expressed with Eq. (2):

154
$$\sqrt{C_i} = \beta_0 + s(u,v) + e_i \quad (2),$$

155   where C_i is the calculated pollutant concentration, β_0 is the overall mean of the

156   response, $s(u,v)$ is the smooth function, and e_i is the residual.

157   **2.2.2. Transport flux assessment**

158   The surface transport fluxes at the Yufa site were calculated with the following

159   formula (White et al., 1976; Wang et al., 2011):

160
$$FLUX = -\sum_{j=1}^{n} C_j \cdot WS_j \cdot cos\theta_j \cdot \sigma^{-1} \quad (3),$$

161
$$f = FLUX \cdot \sigma^{-1} \quad (4),$$

162   where $FLUX$ is the total surface flux of the pollutants ($\mu g\ s^{-1}$); f is surface flux strength

163   of the pollutants, i.e. flux per unit area ($\mu g\ s^{-1}\ m^{-2}$); σ is the cross-sectional area (m^2);

164   C_j is the mean concentration of the pollutants ($\mu g\ m^{-3}$) during the jth observation

165   hour; ϑ_j is the angle between the wind direction and the north–south direction

166   during the jth observation hour; and WS_j is wind speed ($m\ s^{-1}$) during the jth

167   observation hour.

168   Figure S1 shows a schematic diagram of the surface flux calculation. The angle ϑ

169   is the angle between the wind direction and the north–south direction. The direction

170   from south to north (i.e. from the NCP to Beijing) is defined as positive, and that

171   from north to south (i.e. from Beijing to the NCP) as negative. The wind speed and

172   wind direction were assumed to be invariant during the hour (as the hourly mean

173   wind speed and wind direction were used) to evaluate the surface transport fluxes of

174   gaseous pollutants during the observation period.

175   **3. Results and discussion**

176   **3.1. Observations**

177   The time series of hourly average and 24-hour smoothing concentrations of SO_2, NO,

178   NO_2, NO_x, O_3, O_x, and CO observed at the Yufa site from 15 August 2006 to 31

179   October 2008 are shown in Fig. 2. The hourly mean concentrations ($\pm 1\sigma$) of SO_2, NO,

180   NO_2, NO_x, O_3, O_x, and CO were 14 ± 16 ppb, 11 ± 24 ppb, 23 ± 18 ppb, 34 ± 37 ppb, $27\pm$

181   27 ppb, 51 ± 24 ppb, and 1.5 ± 1.3 ppm, respectively, with peak daily average

182   concentrations of 113 ppb, 124 ppb, 190 ppb, 290 ppb, 110 ppb, 191 ppb, and 9.3

183   ppm, respectively. The observed concentrations of these gaseous pollutants were

184   comparable to reported results at the Gucheng site, a polluted rural site to the south-

185   west of Beijing, from July 2006 to September 2007 (Lin et al., 2009). Typical seasonal

186   variations were observed for all gaseous pollutants. Concentrations of primary

187   pollutants, including SO_2, NO, NO_2, NO_x, and CO, were high in winter and low in

188   summer. In contrast, those of secondary pollutants, such as O_3, were high in summer

189   and low in winter.

190   Figure 2. here

191   Meteorological parameters such as WS, RH, T, and BP were also measured at the

192   Yufa site; the monthly statistics are shown in Fig. S2. North (usually in winter) or

193   south wind (usually in summer) prevailed at the Yufa site, with monthly average wind

194   speed mostly below 2 m s^{-1}. It should be clarified here that the North and South

195   wind in Fig. S2 is different from the wind direction definition in meteorology. The

196   South wind in Fig. S2 is the wind with direction from 90° to 270°, while the North

197   wind is from 0° to 90° and from 270° to 360°. Exceptional conditions occurred

198   occasionally in spring and winter for the north wind, with monthly average wind

199   speeds around $2-3$ m s^{-1}. In addition, for the north wind, the mean speed was

200   higher than the median speed, suggesting the prevalence of high wind speeds in

201   both spring and winter. Prevailing north wind with high wind speed during winter

202   and spring has been reported consistently in the Beijing area (Lin, 2008; Wehner et

203   al., 2008). Another exceptional condition occurred in spring for the south wind, with

204   a monthly average wind speed around 2 m s^{-1}. Figure S3 summarises the prevalence

205   of wind direction in the four seasons. Generally, the south wind prevailed in the first

206   half of the year, especially in summer, and the north wind prevailed in the second

207   half of the year, especially in winter. The seasonal variations in RH and T were also

208   typical for Beijing and the NCP, i.e. higher in summer and lower in spring. Surface

209   pressure measurements showed high values in winter and low values in summer due

210   to surface heating and lifting air masses in summer, which partly accounted for the

211   wind field in the NCP (Takegawa et al., 2009).

212   The seasonal variations in gaseous pollutants and meteorological parameters

213   could be linked in certain ways. For example, the high temperature and low pressure

214   in summer suggested a high boundary layer and diluted gaseous pollutants to some

215   extent. The high temperature, light intensity, and relative humidity also favoured the

216   chemical transformation of these primary pollutants and the formation of secondary

217   pollutants. The high wind speeds in spring and winter also affected regional

218   transport, and therefore the concentrations of gaseous pollutants, as discussed

219   below.

3.2. Transport direction

221   As shown in Fig. 1, the Yufa site is located south-west of Beijing city. Prevalent

222   south/south-west or north/north-east wind would bring in polluted or clean air

223   masses, respectively. Air masses from both directions would pass over the Yufa site.

224   Regional transport between the megacity Beijing and the NCP could therefore be

225   observed at the Yufa site. The transport directions for gaseous pollutants, including

226   SO_2, NO, NO_2, NO_x, O_3, O_x, and CO, will be discussed in this section. Bivariate polar

227   plots demonstrating the dependence of pollutant concentrations on wind speed and

228   wind direction were used to investigate the main transport directions. Compared to

229   the nonparametric regression used by Henry et al. (2002), the bivariate polar plot

230   involves the dependence of pollutant concentration on both wind speed and wind

231   direction. The non-linear relationships among the variables (such as concentrations

232   of gaseous pollutants, wind speed, and wind direction) as well as the interactions

233   among these variables can be considered using the GAM method for data smoothing.

234   In addition, the use of polar coordinates makes the graphics more intuitive.

235   Figure 3. here

236   Figure 3a−g show the bivariate polar plots for SO_2, NO, NO_2, NO_x, O_3, O_x, and CO

237   at the Yufa site, respectively. In the low wind speed scenario, high or medium

238   concentrations of NO, NO_2, NO_x, SO_2, and CO were generally observed, along with

239   low O_3 and O_x concentrations. In the high wind speed scenario, the dependence of

240   species concentration on wind speed and wind direction was more varied.

241   Specifically, the bivariate polar plot in Fig. 3b clearly shows dependence of high NO

242   concentration (up to 200 ppb) on low wind speed, with low NO concentration (lower

243   than 5 ppb) at wind speeds >3 m s^{-1}. The bivariate polar plot in Fig. 3c shows similar

244   dependence of high NO_2 concentration on low wind speed, but NO_2 concentrations

245   up to 20 ppb were still observed with medium wind speeds of around 5 m s^{-1} from

246   the south, east, and north-east. Accordingly, the dependence pattern of the NO_x

247   concentration (Fig. 3d) on wind speed and wind direction reflected the features of

248   both NO and NO_2. The dependence pattern of high CO concentration on low wind

249   speed in Fig. 3g was similar to that for NO_x, but a considerable CO concentration,

250   substantially higher than background level, was still observed at wind speeds

251   exceeding 5 m s^{-1} from the south and the east. Figure 3a shows similar dependence

252   of medium-high concentration of SO_2 (around 20 ppb) on low wind speed, with one

253   unique feature being that high SO_2 concentration was observed under conditions of

254   high wind speed, up to 15 m s^{-1}, in various wind directions (especially the south

255   wind). Finally, the bivariate polar plot in Fig. 3e shows the dependence of O_3

256   concentration on wind speed and wind direction, which was somewhat opposite to

257   the patterns for other species. The low O_3 concentration was related to low wind

258   speed or calm wind conditions. With the north wind and medium or high wind

259   speed, a typical background O_3 concentration (around 50 ppb) was observed. With

260   south wind and medium or high wind speed, high O_3 concentration was observed.

261   The dependence of the high O_x concentration on high wind speed from the south

262   and south-east was similar to that of O_3, but no low concentration of O_x was

263   observed under low wind speed conditions, probably due to the compensation of

264   high NO_x concentration at low wind speeds (Fig. 3f).

265   The high concentrations of NO, NO_2, NO_x, and CO and the medium-high

266   concentration of SO_2 observed under low wind speed conditions were consistent

267   with their high emission intensities in the Beijing area. Due to the marked increase in

268   the number of vehicles and heavy energy consumption, Beijing has been a well-

269   known emission hot spot for NO and NO_2 (Tang, 2004). Meanwhile, the extremely

270   high levels of CO emissions in the Beijing area are clearly shown in the emissions

271   map (Fig. S4b) and have been reported consistently (Wang et al., 2011) and directly

272   observed, with peak CO concentrations up to 9.3 ppm. Only medium-high SO_2

273   concentration (~15 ppb) observed even at low wind speed suggested the successful

274   reduction of SO_2 emission, which could be ascribed to the continuous effort of the

275   Chinese government since the 1990s (Tang, 2004). Accordingly, the O_3 concentration

276   under low wind speed conditions was lower than the typical background level, which

277   could be attributed to the rapid titration of O_3 by of accumulation NO.

278   The varied dependence of high pollutant concentrations on high wind speed

279   was obviously due to differences in their transport. Although emission hot spots of

280   NO, NO_2, and NO_x are also widespread in the NCP, the long-range transport of these

281   species to Beijing is limited by the lifetime of these species. The typical lifetime of NO

282   is 42 s, assuming an average O_3 concentration of 50 ppb (Sander et al., 2011). The

283   transport distance of NO is therefore less than 1 km even with a high wind speed of

284   15 m s^{-1}. That is, NO concentration is determined by local emissions rather than

285   regional transport. The high wind speed has a dilution effect on local emissions of

286   species, which accounts for the low NO concentration observed under the high wind

287   speed scenario. NO_2 and NO_x (NO_2+NO) have slightly longer lifetimes in the

288   atmosphere than NO has, typically on the order of several hours (Beirle et al., 2011).

289   Hence, the typical transport distance of these species is around $100-200$ km (Gu et

290   al., 2013). Within such transport distance, the Yufa site is surrounded by various NO_x

291   emission hot spots (Fig. S4a), such as the megacity Beijing to the north, the Baoding–

292   Cangzhou area to the south, and the Tianjin–Tangshan area to the east. It is therefore

293   reasonable to observe the influence of short-range transport, in addition to local

294   emissions, on the local NO_2 and NO_x concentrations. Although our results suggested

295   that short-range transport from these surrounding areas, especially the urban area of

296   Beijing, was a non-negligible factor affecting the local NO_x concentration at the Yufa

297   site, the regional transport of NO_x between Beijing and the NCP is of less significance

298   compared to SO_2 and CO due to its limited transport distance (see below). The

299   oxidation lifetime of CO is typically ~20 days, under the assumption of OH radical

300   concentration of 2×10^6 cm^{-3} (Xu et al., 2011). This is substantially longer than the

301   lifetime of NO_x, making regional transport of CO an important process affecting local

302   air quality in the downwind area. The different lifetimes of CO and NO_x appeared to

303   explain the unique high concentration of CO, but not NO_x, at wind speeds exceeding

304   5 m s^{-1} from the south and the east. Our results suggest that regional transport from

305   the south and central NCP and the Tianjin area could greatly affect local

306   concentrations of CO at the Yufa site and in the Beijing area. Similar to CO, SO_2 has a

307   long lifetime in the atmosphere, i.e. 17 days (Beirle et al., 2014; He et al., 2012), and

308   regional transport of SO_2 was expected to occur. Accordingly, regional transport from

309   emission hot spots located north-east, east, and south of the Yufa site (Fig. S4c), was

310   found to influence the local concentrations of SO_2 (Fig. 3a). Specifically, the

311   highlighted emission hot spots in the central NCP and the south NCP, which

312   accounted for about 70 % of China's coal consumption in 10 % of China's domestic

313   area (China Statistical Yearbook, 2008), is an essential source of SO_2 in the Beijing

314   area by regional transport. Finally, background O_3 levels in the north wind under

315   medium and high speed conditions clearly reflect the transport of background air

316   mass to the Yufa site from locations where the emission intensities of pollutants

317   were relatively low (Fig. S4), whereas O_3 concentrations higher than background level

318   in the south wind under medium and high speed conditions suggest accumulation of

319   O_3 during its transport from the central NCP area or even the south NCP area to the

320   Yufa site. The NCP is known to have high emission intensities of O_3 precursors (Zhang

321   et al., 2014), i.e. NO_x and VOCs. The formation time of O_3 is on the order of several

322   hours, which would facilitate oxidant input to Beijing.

323   In conclusion, the local emissions in the Beijing area closely related to the

324   observed concentrations of NO, NO_2, NO_x, and CO. Regional transport had a clear

325   influence on the concentrations of all gaseous pollutants examined here, with the

326   exception of NO. The emission hot spots located east, north-east, and especially

327   south of the Yufa site determined the regional transport directions from the NCP to

328   the Beijing area. The influence of regional transport differed among species. Regional

329   transport of SO_2, CO, and O_3 from the central and south NCP to the Yufa site were

330   important, whereas regional transport of NO_x was less evident. Factors affecting

331   regional transport included, but were not limited to, the atmospheric lifetime of

332   pollutants, wind field, and local and regional emissions. As the Yufa site is a rural site

333   south of the Beijing area, observation of transport flux there is appropriate in

334   evaluating the transport of pollutants between Beijing and the central and south NCP

335   areas.

336   **3.3. Transport flux**

337   To evaluate the surface transport strengths of the main air pollutants, the surface

338   transport fluxes in the north–south direction were calculated with Eqs. (3) and (4)

339   based on observations at the Yufa site. The cumulative surface flux strengths in

340   each season were also calculated for the 2-year observation period (Table 1). The

341   overall cumulative transport strengths of SO_2, NO, NO_2, NO_x, O_3, O_x, and CO were

342   92.6, −62.2, −8.9, −71.0, 217.3, 213.8, and 1038.1 mg s^{-1} m^{-2} during the observation

343   period from 01 September 2007 to 31 August 2008. The results suggested that the

344   transport direction of SO_2, O_3, O_x, and CO was from the NCP to the megacity Beijing,

345   whereas that of NO, NO_2, and NO_x was from the megacity Beijing to the NCP.

346   Table 1. here

347   To understand the transport fluxes reported here, it is necessary to discuss the

348   affecting factors. First, the prevalent wind is a dominant factor affecting the surface

349   fluxes. Figure 4 shows the time series of daily average surface flux strength, i.e. flux

350   per unit cell (μg s^{-1} m^{-2}) of SO_2, NO, NO_2, NO_x, O_3, O_x, and CO, and corresponding

351   wind vectors (m s^{-1}) during the observation period. In general, the variations in the

352   pollutant flux strengths showed a saw-toothed pattern, with positive (from the NCP

353   to Beijing) and negative (from Beijing to the NCP) fluxes prevailing according to the

354   shift in wind direction. Meanwhile, mainly due to the seasonal variations in wind

355   speed and wind direction (Figs. S2 and S3), the magnitude of surface fluxes showed

356   similar seasonal variation (Table 1). High positive fluxes were observed in summer,

357   and high negative fluxes in winter. As the north wind prevailed significantly over the

358   south wind in winter, and the south wind over the north wind in summer, the

359   cumulative values of fluxes in these two seasons were the highest. During the other

360   two seasons, frequent changes in positive and negative fluxes tended to cancel

361   each other out, making the cumulative fluxes less significant. This dominant role of

362   wind field could also be illustrated by conditions during the winter of 2006.

363   Exceptionally, the south wind prevailed in the winter of 2006 (Fig. S3b), leading to

364   unusual positive fluxes of pollutants (Table 1).

365   Figure 4. here

366   Second, the transport flux is determined not only by the wind field but also by

367   the emissions of pollutants in the upwind area. Various pollutants showed different

368   patterns of seasonal variations in flux as a result of relative emission strengths in

369   the upwind area compared to local emissions (Fig. S4). For example, the seasonal

370   cumulative fluxes of SO_2 were mainly positive, except in winter. The significant

371   regional transport of SO_2 from the NCP to Beijing in all seasons except winter could

372   be partly attributed to the high emission intensity of SO_2 in the NCP and the

373   reduction of SO_2 emission in Beijing, whereas the SO_2 flux output from Beijing was

374   determined by the prevalent north wind, as explained above. In contrast to the

375   positive input flux of SO_2, the seasonal cumulative fluxes of CO were negative in

376   both winter and autumn. The small output flux of CO in autumn reflected increased

377   CO emission in Beijing, which was sufficiently strong to account for the strong CO

378   emissions in the NCP. The influence of emissions on transport flux could also be

379   inferred from an emissions-reduction scenario. For example, the concentrations of

380   pollutants in the summer of 2008 (Olympics year) were substantially lower (Fig. 2),

381   which was ascribed to the significant reduction in emissions both in the Beijing area

382   and the NCP during the period of the 2008 Beijing Olympics (Streets et al., 2007).

383   The emissions reduction in the NCP during the summer of 2008 led to lower fluxes

384   than were seen in the summer of 2007 (Table 1).

385   Finally, the chemical properties of these species could also affect the flux.

386   Although both Beijing and the NCP are regarded as emissions hot spots for O_3

387   precursors, the short distance between Beijing and the Yufa site may hinder the

388   secondary formation of O_3 to some extent. This could lead to underestimation of

389   transport strength from Beijing to the NCP. In contrast, the marked influence of NO_x

390   emissions in the Beijing area on local concentrations may lead to an overestimate of

391   the transport strength of NO_x from Beijing to the NCP.

392   Overall, the transport fluxes are influenced by at least the wind field,

393   emissions inventory in both the upwind and local areas, and the chemical fates of

394   these pollutants in the atmosphere. These observations provide insight for the

395   analysis of projected transport flux under various emissions-reduction scenarios in

396   the future. On the other hand, the dependence of the fluxes on these factors,

397   which can vary, suggests that the fluxes reported here should not be compared with

398   other reports under different conditions. Indeed, the flux calculations here in mg s^{-1}

399   m^{-2} provide only a measurement of the regional transport strength, but cannot be

400   considered as absolute values, as reported in the literature (An et al., 2007; Wang

401   et al., 2011). The limitation of surface fluxes discussed here could also be suggested

402   by the nature of flux observation. For example, our calculations did not consider

403   the fluxes at high altitudes or at the boundary layer height. Both wind field and

404   concentrations of pollutants could be different at high altitudes (He et al., 2012).

405   Furthermore, the location of the observation station at the Yufa site also had an

406   influence on the flux observations. As the transport distance of pollutants is a

407   significant factor, the fluxes between the NCP and Beijing calculated in this study

408   cannot be applied to other sites. For example, a previous study at the Gucheng site

409   indicated positive fluxes of NO_x (Lin et al., 2009), whereas in our study, negative

410   fluxes were consistently observed.

411   Furthermore, as the wind field, emissions inventory, and atmospheric

412   lifetimes of pollutants were taken into consideration, it was concluded that SO_2, CO,

413   and the oxidant input from NCP to Beijing were substantial. It should be noted that

414   the semi-basin topography of the megacity Beijing, which is surrounded by

415   mountains to the west and north, also magnified the influence of pollutant

416   transport from the NCP by favouring their accumulation (Lin et al., 2011).

417   **4. Conclusions**

418   We used 2-year observation data at a rural site south of Beijing to investigate

419   regional transport of pollutants between the megacity Beijing and the NCP as part of

420   the "Campaign of Air Quality Research in Beijing and Surrounding Region 2006–

421   2008" (CAREBeijing 2006–2008). The gaseous pollutants SO_2, NO, NO_2, NO_x, CO, and

422   O_3, together with meteorological data, were determined at Yufa from August 2006 to

423   October 2008. During the observation period, the average concentrations of the

424   pollutants at the Yufa site were relatively high, suggesting a profound influence of the

425   emissions from the megacity Beijing and regional transport from the NCP. Through

426   bivariate polar plots, we found that the south wind, at relatively high wind speed,

427   was essential for the inflow of SO_2, CO, and O_3 to Beijing. The seasonal variations in

428   the transport fluxes highlighted the strong inflow transport in summer with outflow

429   transport in winter for Beijing, mainly varying with the prevailing wind. Our results

430   again suggested that Beijing and the NCP have tight interactions through regional

431   transport of air pollutants. Factors affecting the transport flux such as meteorological

432   parameters, especially wind speed and wind direction, emissions inventory, and

433   photochemical reactions are essential for the regional transport fluxes and thus the

434   air quality of the megacity Beijing and its surrounding areas. Therefore, both local

435   emissions reduction and regional cooperative control should be taken considered in

436   air quality management of Beijing.

437   **Author contribution**. T. Zhu designed the experiments and L. Zeng and the staff of

438   the Yufa site carried out the experiment. Y. Li conducted the data analysis with

439   contributions from all co-authors. J. Liu provided the emission maps. J. Wang

440   managed the observation data of the program. Y. Li prepared the manuscript with

441   the help of T. Zhu, C. Ye, J. Liu and Y. Zhu.

442   **Data availability.** The observation data of the Yufa site used in this paper is available

443   on requests.

Acknowledgements. The authors express their sincere thanks to the staff of the Yufa

site for carrying out the measurements. This work as part of CAREBeijing (Campaign

of Atmospheric Researches in Beijing and surrounding area) was supported by Beijing

Council of Science and Technology. This study was also supported by the National

Natural Science Foundation Committee of China (21190051, 41121004, 41421064),

the European 7th Framework Programme Project PURGE (265325), the Collaborative

Innovation Center for Regional Environmental Quality.

The English in this document has been checked by at least two professional editors,

both native speakers of English. For a certificate, please see:

http://www.textcheck.com/certificate/KcBduS

References

An, X., Zhu, T., Wang, Z., Li, C., and Wang, Y.: A modeling analysis of a heavy air
    pollution episode occurred in Beijing, Atmos. Chem. Phys., 7, 3103-3114, doi:
    10.5 194/acp-7-3103-2007, 2007.

Beirle, S., Boersma, K. F., Platt, U., Lawrence, M. G., and Wagner, T.: Megacity
    emissions and lifetimes of nitrogen oxides probed from space, Science, 333,
    1737-1739, doi:10.1126/science.1207824, 2011.

Beirle, S., Hörmann, C., Penning de Vries, M., Dörner, S., Kern, C., and Wagner, T.:
    Estimating the volcanic emission rate and atmospheric lifetime of SO_2 from
    space: a case study for Kīlauea volcano, Hawai`i, Atmos. Chem. Phys., 14, 8309-
    8322, doi:10.5194/acp-14-8309-2014, 2014.

Carslaw, D. C., Beevers, S. D., Ropkins, K., and Bell, M. C.: Detecting and quantifying
    aircraft and other on-airport contributions to ambient nitrogen oxides in the
    vicinity of a large international airport, Atmos. Environ., 40, 5424-5434, 2006.

470   China Statistical Yearbook 2008 (Beijing: China Statistic Press) (in Chinese).

471   Gu, D., Wang, Y., Smeltzer, C., and Liu, Z.: Reduction in NOx Emission Trends over
472   China: Regional and Seasonal Variations, Environ. Sci. Technol., 47, 12912-
473   12919, doi:10.1021/es401727e, 2013.

474   Guo, S., Hu, M., Wang, Z. B., Slanina, J., and Zhao, Y. L.: Size-resolved aerosol water-
475   soluble ionic compositions in the summer of Beijing: implication of regional
476   secondary formation, Atmos. Chem. Phys., 10, 947-959, doi:10.5194/acp-10-
477   947-2010, 2010.

478   He, H., Li, C., Loughner, C. P., Li, Z., Krotkov, N. A., Yang, K., Wang, L., Zheng, Y., Bao,
479   X., Zhao, G., and Dickerson, R. R.: SO_2 over central China: Measurements,
480   numerical simulations and the tropospheric sulfur budget, J. Geophys. Res.-
481   Atmos., 117, D00K37, doi:10.1029/2011JD016473, 2012.

482   Henry, R. C., Chang, Y.-S., and Spiegelman, C. H.: Locating nearby sources of air
483   pollution by nonparametric regression of atmospheric concentrations on wind
484   direction, Atmos. Environ., 36, 2237-2244, 2002.

485   Jayamurugan, R., Kumaravel, B., Palanivelraja, S., and Chockalingam, M. P.: Influence
486   of Temperature, Relative Humidity and Seasonal Variability on Ambient Air
487   Quality in a Coastal Urban Area, International Journal of Atmospheric Sciences,
488   2013, 1-7, doi:10.1155/2013/264046, 2013.

489   Lin, W., Xu, X., Zhang, X., and Tang, J.: Contributions of pollutants from North China
490   Plain to surface ozone at the Shangdianzi GAW Station, Atmos. Chem. Phys., 8,
491   5889-5898, doi:10.5194/acp-8-5889-2008, 2008.

492   Lin, W., Xu, X., Ge, B., and Zhang, X.: Characteristics of gaseous pollutants at
493   Gucheng, a rural site southwest of Beijing, J. Geophys. Res., doi:114, 10.1029/
494   2008jd010339, 2009.

495   Lin, W., Xu, X., Ge, B., and Liu, X.: Gaseous pollutants in Beijing urban area during the
496   heating period 2007–2008: variability, sources, meteorological, and chemical
497   impacts, Atmos. Chem. Phys., 11, 8157-8170, doi:10.5194/acp-11-8157-2011,
498   2011.

499   Matsui, H., Koike, M., Kondo, Y., Takegawa, N., Kita, K., Miyazaki, Y., Hu, M., Chang, S.
500   Y., Blake, D. R., Fast, J. D., Zaveri, R. A., Streets, D. G., Zhang, Q., and Zhu, T.:
501   Spatial and temporal variations of aerosols around Beijing in summer 2006:
502   Model evaluation and source apportionment, J. Geophys. Res.-Atmos.,114,
503   D00G13, doi:10.1029/2008JD010906, 2009.

504 Parrish, D. D., and Zhu, T.: Clean Air for Megacities, Science, 326, 674-675,
505   doi:10.1126/science.1176064, 2009.

506 Shao, M., Tang, X., Zhang, Y., and Li, W.: City Clusters in China: Air and Surface Water
507   Pollution, Front. Ecol. Environ., 4, 353-361, 2006.

508 Sander, S. P., J. Abbatt, J. R. Barker, J. B. Burkholder, R. R. Friedl, D. M. Golden, R. E.
509   Huie, C. E. Kolb, M. J. Kurylo, G. K. Moortgat, V. L. Orkin and P. H. Wine
510   "Chemical Kinetics and Photochemical Data for Use in Atmospheric Studies,
511   Evaluation No. 17," JPL Publication 10-6, Jet Propulsion Laboratory, Pasadena,
512   2011 http://jpldataeval.jpl.nasa.gov.

513 Streets, D. G., Fu, J. S., Jang, C. J., Hao, J., He, K., Tang, X., Zhang, Y., Wang, Z., Li, Z.,
514   Zhang, Q., Wang, L., Wang, B., and Yu, C.: Air quality during the 2008 Beijing
515   Olympic Games, Atmos. Environ., 41, 480-492,2007.

516 Takegawa, N., Miyakawa, T., Kuwata, M., Kondo, Y., Zhao, Y., Han, S., Kita, K., Miyazaki,
517   Y., Deng, Z., Xiao, R., Hu, M., van Pinxteren, D., Herrmann, H., Hofzumahaus, A.,
518   Holland, F., Wahner, A., Blake, D. R., Sugimoto, N., and Zhu, T.: Variability of
519   submicron aerosol observed at a rural site in Beijing in the summer of 2006, J.
520   Geophys. Res., 114, D00G05, doi:10.1029/2008jd010857, 2009.

521 Tang, X. Y. (2004), The characteristics of urban air pollution in China, in Urbanization,
522   Energy, and Air Pollution in China, pp. 47–54, Natl. Acad. Press, Washington, D.
523   C.

524 Wang, M., Zhu, T., Zheng, J., Zhang, R. Y., Zhang, S. Q., Xie, X. X., Han, Y. Q., and Li, Y.:
525   Use of a mobile laboratory to evaluate changes in on-road air pollutants during
526   the Beijing 2008 Summer Olympics, Atmos. Chem. Phys., 9, 8247-8263,
527   doi:10.5194/acp-9-8247-2009, 2009.

528 Wang, M., Zhu, T., Zhang, J. P., Zhang, Q. H., Lin, W. W., Li, Y., and Wang, Z. F.: Using a
529   mobile laboratory to characterize the distribution and transport of sulfur dioxide
530   in and around Beijing, Atmos. Chem. Phys., 11, 11631-11645, doi:10.5194/acp-
531   11-11631-2011, 2011.

532 Wang, T., Ding, A., Gao, J., and Wu, W. S.: Strong ozone production in urban plumes
533   from Beijing, China, Geophys. Res. Lett., 33, L21806, doi:10.1029/2006GL02
534   7689, 2006.

535 Wehner, B., Birmili, W., Ditas, F., Wu, Z., Hu, M., Liu, X., Mao, J., Sugimoto, N., and
536   Wiedensohler, A.: Relationships between submicrometer particulate air
537   pollution and air mass history in Beijing, China, 2004–2006, Atmos. Chem. Phys.,
538   8, 6155-6168, doi:10.5194/acp-8-6155-2008, 2008.

539 Westmoreland, E. J., Carslaw, N., Carslaw, D. C., Gillah, A., and Bates, E.: Analysis of
540   air quality within a street canyon using statistical and dispersion modelling
541   techniques, Atmos. Environ., 41, 9195-9205, 2007.

542 Wu, Q. Z., Wang, Z. F., Gbaguidi, A., Gao, C., Li, L. N., and Wang, W.: A numerical
543   study of contributions to air pollution in Beijing during CAREBeijing-2006,
544   Atmos. Chem. Phys., 11, 5997-6011, doi:10.5194/acp-11-5997-2011, 2011.

545 Xu, J., Ma, J. Z., Zhang, X. L., Xu, X. B., Xu, X. F., Lin, W. L., Wang, Y., Meng, W., and Ma,
546   Z. Q.: Measurements of ozone and its precursors in Beijing during summertime:
547   impact of urban plumes on ozone pollution in downwind rural areas, Atmos.
548   Chem. Phys., 11, 12241-12252, doi:10.5194/acp-11-12241-2011, 2011.

549 Xu, X., Zhou, L., Zhou, X., Yan, P., Weng, Y., Tao, S., Mao, J., Ding, G., Bian, L., and Jhon,
550   C.: Influencing domain of peripheral sources in the urban heavy pollution
551   process of Beijing, Science in China, 48, 565-575, 2005.

552 Yuan, Z., Lau, A. K. H., Shao, M., Louie, P. K. K., Liu, S. C., and Zhu, T.: Source analysis
553   of volatile organic compounds by positive matrix factorization in urban and rural
554   environments in Beijing, J. Geophys. Res., 114, 10.1029/2008 jd011190, 2009.

555 Zhang, J. P., Zhu, T., Zhang, Q. H., Li, C. C., Shu, H. L., Ying, Y., Dai, Z. P., Wang, X., Liu,
556   X. Y., Liang, A. M., Shen, H. X., and Yi, B. Q.: The impact of circulation patterns on
557   regional transport pathways and air quality over Beijing and its surroundings,
558   Atmos. Chem. Phys., 12, 5031-5053, 10.5194/acp-12-5031-2012, 2012.

559 Zhang, Q., Yuan, B., Shao, M., Wang, X., Lu, S., Lu, K., Wang, M., Chen, L., Chang, C.
560   C., and Liu, S. C.: Variations of ground-level O_3 and its precursors in Beijing in
561   summertime between 2005 and 2011, Atmos. Chem. Phys., 14, 6089-6101,
562   doi:10.5194/acp-14-6089-2014, 2014.

563 Zhu, L., Huang, X., Shi, H., Cai, X., and Song, Y.: Transport pathways and potential
564   sources of PM_{10} in Beijing, Atmos. Environ., 45, 594-604, 2011.

565

566

567

568
569
570

571   **Table.1.** The overall and seasonal cumulitive flux strength (mg s^{-1} m^{-2}) of gaseous

572   pollutants at the Yufa site from 1 September 2006 to 31 August 2008.

f (mg s^{-1} m^{-2})	SO_2	NO	NO_2	NO_x	CO	O_3	O_x
Spring 2007	19.2	-3.3	0.1	-3.2	77.4	5.8	5.9
Spring 2008	28.2	-3.7	0.5	-3.2	330.4	22.4	22.8
Summer 2007	19.7	0.7	15	15.6	1074.2	127.3	142.3
Summer 2008	11	0.2	2	2.2	230	92.3	94.2
Autumn 2006	9.5	-8.6	-4.1	-12.8	-58.2	33.8	35.3
Autumn 2007	11	-11.5	-6.1	-17.5	-108.7	17.5	11.5
Winter 2006	21	-12.3	6.4	-5.8	630.8	-21.1	-14.7
Winter 2007	-26.9	-23.7	-22.7	-46.4	-1137.9	-60.7	-83.4
Total	92.6	-62.2	-8.9	-71	1038.1	217.3	213.8

573

574

575   Figure Captions

576   Figure 1. The location information of the Yufa site.

577   Figure 2. Time series of hourly mean (black line) and 24-hour smoothing (red line)

578   concentrations of SO_2, NO, NO_2, NO_x, O_3, O_x and CO at the Yufa site from 15

579   August 2006 to 31 October 2008.

580   Figure 3. Bivariate polar plots for SO_2 (a), NO (b), NO_2 (c), NO_x (d), O_3 (e), O_x (f) and CO

581   (g) concentrations based on hourly average data at the Yufa site from 1

582   September 2006 to 31 August 2008. The colour scale shows the

583   concentrations of pollutants in ppb (or ppm specially for CO) and the radial

584   scale shows the wind speed (m s^{-1}), which increases from the centre of the

585   plot radially outwards.

586   Figure 4. Time series of surface flux strength (i.e. flux per unit cell, µg s^{-1} m^{-2} or mg s^{-}

587   ^{1} m^{-2}) for SO2, NO, NO2, NOx, O3, Ox, CO and wind vector , i.e.

588             $-\sum_{j=1}^{n} WS_j \cdot cos\theta_j$ (WSVECTOR, m s^{-1}) based on daily average data at the

589   Yufa site from 15 August 2006 to 31 October 2008. The red shaded line

590   indicates the positively transport direction of gaseous pollutants from

591   south to north (i.e. from the NCP to Beijing) and the black shaded line

592   represents the negatively transport direction of gaseous pollutants from

593   north to south (i.e. from Beijing to the NCP).

594

595

596

597

598

599

600   Figure 1. The location information of the Yufa site.

601

602
603
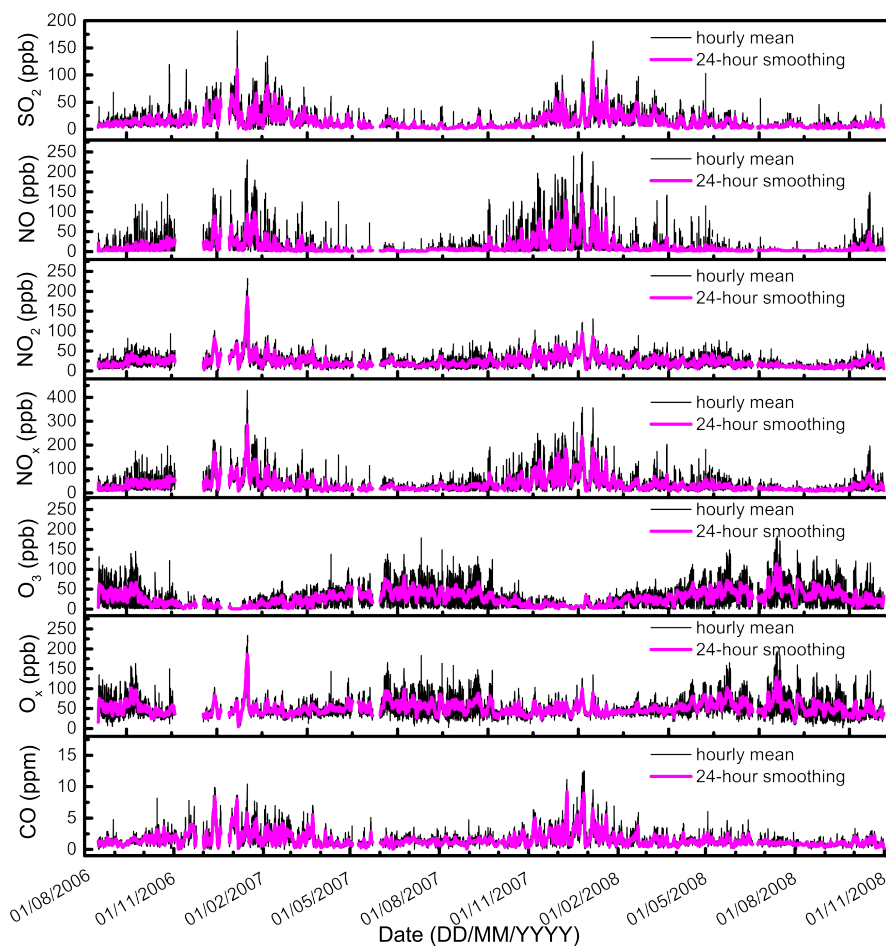
604
605   Figure 2. Time series of hourly mean (black line) and 24-hour smoothing (red line)

606   concentrations of SO_2, NO, NO_2, NO_x, O_3, O_x and CO at the Yufa site from 15 August

607   2006 to 31 October 2008.

608

609

610

611
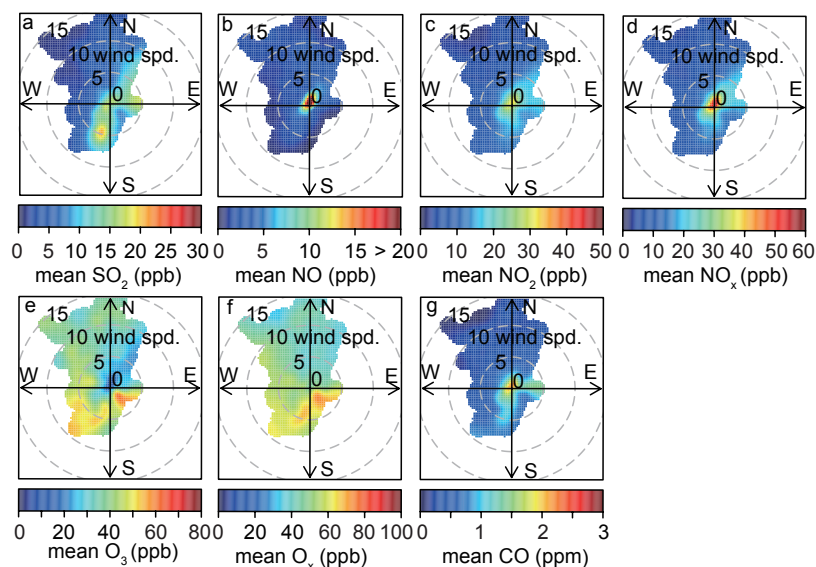
612

613 Figure 3. Bivariate polar plots for SO_2 (a), NO (b), NO_2 (c), NO_x (d), O_3 (e), O_x (f) and CO

614 (g) concentrations based on hourly average data at the Yufa site from 1 September

615 2006 to 31 August 2008. The colour scale shows the concentrations of pollutants in

616 ppb (or ppm specially for CO) and the radial scale shows the wind speed (m s^{-1}),

617 which increases from the centre of the plot radially outwards.
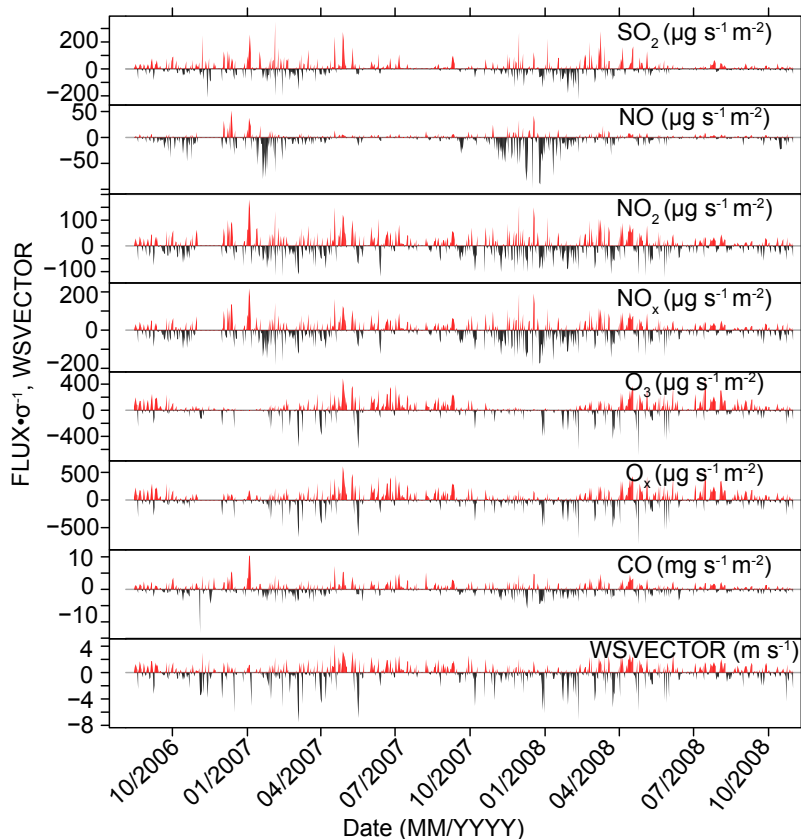
618

619 Figure 4. Time series of surface flux strength (i.e. flux per unit cell, $\mu g\ s^{-1}\ m^{-2}$ or $mg\ s^{-}$

620 $^{1}\ m^{-2}$) for SO_2, NO, NO_2, NO_x, O_3, O_x, CO and wind vector, i.e. $-\sum_{j=1}^{n} WS_j \cdot cos\theta_j$

621 (WSVECTOR, $m\ s^{-1}$) based on daily average data at the Yufa site from 15 August 2006

622 to 31 October 2008. The red shaded line indicates the positively transport direction

623 of gaseous pollutants from south to north (i.e. from the NCP to Beijing) and the black

624 shaded line represents the negatively transport direction of gaseous pollutants from

625 north to south (i.e. from Beijing to the NCP).

626